Electrotonic Coupling between Human Atrial Myocytes and Fibroblasts Alters Myocyte Excitability and Repolarization

Mary M. Maleckar,[†‡] Joseph L. Greenstein,[†‡] Wayne R. Giles,[§] and Natalia A. Trayanova[†‡*]
[†]Department of Biomedical Engineering and [‡]Institute for Computational Medicine, Johns Hopkins University, Baltimore, Maryland; and
[§]Faculty of Kinesiology, University of Calgary, Calgary, Alberta, Canada

ABSTRACT Atrial fibrosis has been implicated in the development and maintenance of atrial arrhythmias, and is characterized by expansion of the extracellular matrix and an increased number of fibroblasts (Fbs). Electrotonic coupling between atrial myocytes and Fbs may contribute to the formation of an arrhythmogenic substrate. However, the role of these cell-cell interactions in the function of both normal and diseased atria remains poorly understood. The goal of this study was to gain mechanistic insight into the role of electrotonic Fb-myocyte coupling on myocyte excitability and repolarization. To represent the system, a human atrial myocyte (hAM) coupled to a variable number of Fbs, we employed a new ionic model of the hAM, and a variety of membrane representations for atrial Fbs. Simulations elucidated the effects of altering the intercellular coupling conductance, electrophysiological Fb properties, and stimulation rate on the myocyte action potential. The results demonstrate that the myocyte resting potential and action potential waveform are modulated strongly by the properties and number of coupled Fbs, the degree of coupling, and the pacing frequency. Our model provides mechanistic insight into the consequences of heterologous cell coupling on hAM electrophysiology, and can be extended to evaluate these implications at both tissue and organ levels.

INTRODUCTION

Atrial fibrosis increases with age and develops in conjunction with cardiomyopathy and heart failure, and has been linked to an increased incidence of rhythm disturbances, including atrial fibrillation (AF) (1). An increased and heterogeneous fibrillar architecture has been implicated as having both structural and functional roles in the development and maintenance of AF (2).

Fibrosis is characterized by both an expansion of the extracellular matrix (ECM) surrounding cardiomyocytes (3) and an increase in the number of cardiac fibroblasts (Fbs) (4,5). A number of studies have suggested that increased ECM deposition may alter or inhibit conduction (6–8), contributing to the generation and maintenance of reentrant waves (9,10). However, the mechanisms by which fibrosis contributes to atrial arrhythmias remain to be completely characterized. Recent in vitro studies have revealed that cardiac Fbs form functional gap junctions with myocytes (4,5,11) that can modify impulse conduction (12,13). These results suggest a potential role for Fb-myocyte coupling (FMC) in atrial arrhythmias. However, because in situ studies employing direct experimental techniques currently present several methodological difficulties (14), a comprehensive understanding of the impact of heterologous cell coupling in atrial arrhythmogenesis has not yet been achieved.

Cardiac Fbs are nonexcitable cells that are responsible for the synthesis and maintenance of the ECM, which surrounds and supports cardiomyocytes. However, it is now known that Fbs can express voltage-dependent ion channels. For example, intrinsic K^+ channels contribute to a resting potential in isolated Fbs that is less negative than that of cardiomyocytes (15,16). Fbs have thus been proposed to function as both a current source and sink when coupled to myocytes (13,14,17–19).

Recent computational studies have investigated the role of FMC in the human ventricular action potential (AP) (20), the possible role of Fbs in generating pacemaker activity (21), the impact of FMC on impulse propagation in a strand of murine ventricular myocytes (19), and the loading effects of FMC on the resting membrane potential (RMP), impulse propagation, and repolarization in canine myocytes (18). Among the interesting implications of FMC are depolarization of the myocyte RMP (13,18), decreased AP amplitude (APA), reduced excitability (18,22), and decreases in conduction and maximum upstroke velocities (22).

Several unanswered questions, however, remain with respect to understanding the effects of FMC in atrial electrophysiology. In large part, this is because coupling effects on AP morphology are tissue- and thus myocyte model-dependent (18,19). FMC in the human atrium has not yet been explored. However, FMC may prove especially influential in the repolarization of human atrial myocytes (hAMs) because of their small cell capacitance and diminished repolarization reserve. In addition, the contribution of differences between atrial and ventricular Fbs (15,16,23,24) to changes in the AP dynamics of coupled myocytes has not been characterized. Finally, how FMC affects the electrophysiology of the hAM at a variety of physiological rates remains unknown, hindering characterization of the potential role of FMC in atrial rhythm disturbances.

The main goal of this study was to explore the effects of FMC on myocyte excitability and repolarization. To that end, we conducted numerical simulations of the coupled

Submitted December 30, 2008, and accepted for publication July 31, 2009.

*Correspondence: ntrayanova@jhu.edu

Editor: Dorothy A. Hanck.

0006-3495/09/10/2179/12 $2.00

doi: 10.1016/j.bpj.2009.07.054

Fb-hAM system, employing a new model of the adult hAM (25) as well as new membrane models of the atrial Fb. Specifically, we investigated the effects of changes in 1), the intercellular coupling conductance; 2), the electrophysiological Fb properties; 3), the number of coupled Fbs; and 4), the stimulation rate on hAM AP dynamics. The results provide mechanistic insight into the consequences of FMC on hAM electrophysiology.

MATERIALS AND METHODS

Cell-cell coupling

Fbs surround cardiomyocytes in normal tissue, such that each myocyte is associated with at least one Fb (4). The exact Fb/myocyte ratio in atrial tissue remains unknown, but it may increase with fibrotic remodeling. Homologous coupling between Fbs may also occur. However, because this study focused primarily on the effects of FMC on the AP dynamics of the hAM, only heterologous cell connections were considered (see Discussion).

To incorporate a range of numbers of coupled Fbs, one to three Fbs were coupled through a linear, fixed resistance (G_{gap}) to a single hAM (Fig. 1 *A*). Experimental studies have reported a range of possible G_{gap} values between Fbs and myocytes (26). In this study, G_{gap} was set at one of two values: 0.5 or 8.0 nS ("Low" or "High" G_{gap}, respectively), corresponding to the low and high ends of the range of G_{gap} values between Fb-myocyte pairs measured experimentally (13,26).

The paradigm of electrotonic coupling between the hAM and several Fbs is illustrated in Fig. 1 *B*. The membrane potential of the myocyte is governed by the following differential equation:

$$dV_{myo}/dt = -\left(1/C_{m,myo}\right)\left[I_{myo}\left(V_{myo},t\right) + I_{stim} + \sum_{i=1:n} I_{gap}\right] \quad (1)$$

where V_{myo} is the transmembrane potential of the hAM, $C_{m,\ myo}$ is the membrane capacitance of the myocyte, I_{myo} is the net membrane current of the myocyte, I_{stim} is the stimulus current applied to the myocyte membrane, and I_{gap} is the current that flows through the gap junction between the myocyte and each Fb. Unlike previous formulations (20), the formulation presented here accounts for the movement of Na^+ and K^+ ions through the gap junction between each Fb and the hAM (provided that the Fb membrane incorporates active conductances). As such, the formulation for the I_{gap} of each gap junction is governed by a pair of equations that account for the movement of Na^+ and K^+ as separate ionic species, known as the assumption of independence:

$$I_{gap,K} = G_{gap,K}\left[\left(V_{myo} - V_{Fb}\right) - E_{K,gap}\right] \quad (2)$$

$$I_{gap,Na} = G_{gap,Na}\left[\left(V_{myo} - V_{Fb}\right)E_{Na,gap}\right] \quad (3)$$

$$I_{gap} = I_{gap,K} + I_{gap,Na} \quad (4)$$

where $I_{gap,K}$ and $I_{gap,Na}$ are the gap junctional currents attributable to K^+ and Na^+, respectively, and V_{Fb} is the transmembrane potential of the Fb. The variables $E_{K,gap}$ and $E_{Na,gap}$ are the reversal potentials across the gap junction for K^+ and Na^+, respectively:

$$E_{K,gap} = RT/F\log\left(\left[K^+\right]_{i,\ Fb}/\left[K^+\right]_{i,myo}\right) \quad (5)$$

$$E_{na,gap} = RT/F\log\left(\left[Na^+\right]_{i,\ Fb}/\left[Na^+\right]_{i,myo}\right) \quad (6)$$

where R is the universal gas constant; T is the temperature in Kelvin; F is Faraday's constant; $[K^+]_{i,\ Fb}$ and $[K^+]_{i,\ myo}$ are the intracellular concentrations of K^+ in the Fb and myocyte, respectively; and $[Na^+]_{i,Fb}$ and $[Na^+]_{i,myo}$ are the intracellular concentrations of Na^+ in the Fb and myocyte, respectively.

Because it is still unclear what role active conductances in the Fb membrane may play during FMC, additional simulations were conducted

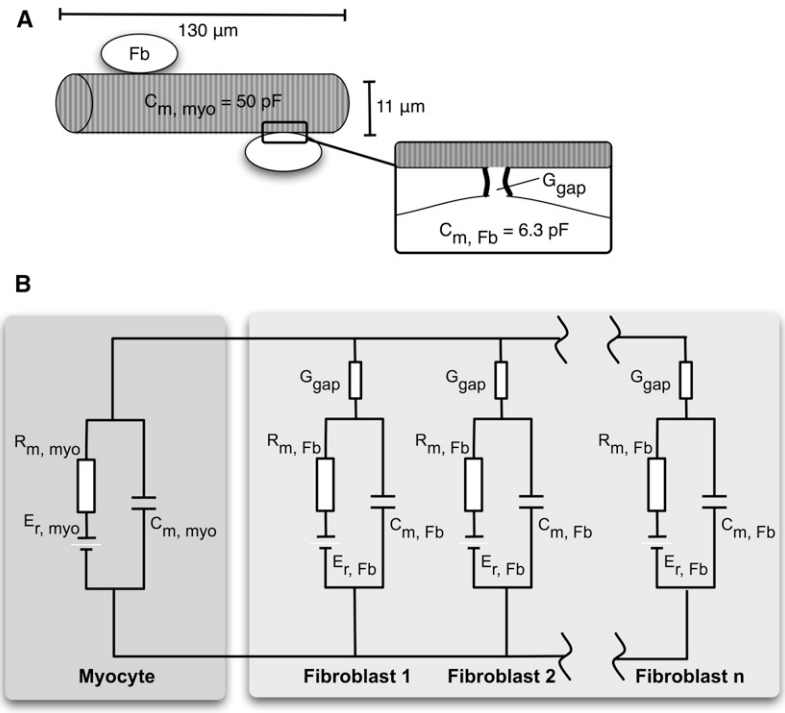

FIGURE 1 A schematic representation of FMC. (*A*) A hAM (myo) is coupled to a number n of identical Fbs via an ohmic gap junctional conductance (G_{gap}) of 0.5 or 8 nS. The membrane capacitance of the myocyte ($C_{m,\ myo}$) is 50 pF, and the membrane capacitance of each Fb ($C_{m,\ Fb}$) is 6.3 pF. (*B*) Equivalent circuit model of FMC, where R_m represents the membrane resistance of a single cell. Fbs are represented by either an RC circuit (Passive model) or an Active membrane model with $V_{rest,\ Fb}$ either −47.8 mV (Active 1) or −31.4 mV (Active 2). E_r is the reversal potential.

assuming a passive Fb membrane resistance. In this case, no specific ion species was assigned as the charge carrier for I_{gap}, which is defined as:

$$I_{gap} = G_{gap}(V_{myo} - V_{Fb}) \quad (7)$$

The differential equation governing V_{Fb} is:

$$dV_{Fb}/dt = -(1/C_{m,Fb})[I_{Fb}(V_{Fb},t) - I_{gap}] \quad (8)$$

where $C_{m,Fb}$ is the membrane capacitance of the Fb, and I_{Fb} is the net membrane current of the Fb.

Model of the hAM

Because in this study we sought to investigate the effects of electrotonic FMC interactions on the excitability and repolarization of the hAM, we believed it was essential to use a hAM ionic model that accurately represents atrial AP dynamics. We therefore employed a new model of the adult hAM, which is described in detail elsewhere (25). The model is computationally efficient and incorporates physiologically accurate repolarization processes. In addition, the model correctly replicates APD restitution of the adult hAM, a requirement for any investigation that employs a variety of pacing rates.

Electrophysiological models of atrial Fbs

Because the role played by active conductances in the Fb membrane during FMC is still unclear, we employed two types of electrophysiological models of the atrial Fb. The first was a "passive" electrical model in which a membrane capacitance, $C_{m,Fb}$, is connected in parallel with a linear resistance, $R_{m,Fb}$. The value of $C_{m,Fb}$ was chosen to be 6.3 pF and $R_{m,Fb}$ was set at 10.7 GΩ (15,20). This formulation is termed the Passive model of the atrial Fb.

The second type of electrophysiological model used to describe the atrial Fb was based on the general formulation of MacCannell et al. (20) and modified to represent atrial Fb properties (a complete description of this model can be found in the Supporting Material). The value of $C_{m,Fb}$ was again chosen to be 6.3 pF (15,20). The RMP of the atrial Fb for this active model is −47.8 mV, within the range of experimentally recorded values (15,16). This model will be referred to as the *Active 1* model of the atrial Fb.

It was recently suggested that the RMP of an Fb can have a significant influence on the electrophysiological behavior of the coupled myocyte (14,18,19). Because a variety of Fb RMPs have been recorded in experiments (11,15,16,24,27), a second active model of the atrial Fb with a less negative RMP was developed. This was achieved via a shift of the voltage dependence of the steady-state activation and inactivation of the time- and voltage-dependent K^+ current, I_{Kv}, by +20 mV (a complete description of this model can be found in the Supporting Material). The RMP of the atrial Fb for this second active model is −31.4 mV, which is also an experimentally recorded value (26,28). This model will be referred to as the *Active 2* model of the atrial Fb.

Stimulation protocol and data analysis

In the human atria, a variety of myocyte activation rates may occur as a result of vagal or adrenergic stimulation, tachyarrhythmias, and/or pathological remodeling. To investigate the role of pacing rate, we paced the coupled system at frequencies of 0.5, 1, 1.33, 2, 2.67, or 4 Hz (corresponding to basic cycle lengths of 2000, 1000, 750, 500, 375, and 250 ms, respectively) for each selected value of G_{gap} (0.0 (control), 0.5, or 8.0 nS) and for each number of coupled Fbs (1–3) represented by the Passive, Active 1, or Active 2 model. APs were initiated by a −5.6 pA/pF current injection of 6 ms duration, which was assumed to be carried by K^+ ions (25,29). Stimulation was continued for a minimum of 1000 cycles to ensure that the coupled system had reached steady state. The results correspond to the last cycle in each simulation.

The peak value of the fast sodium current ($I_{Na,peak}$) was recorded for each AP. Analysis of the results also included a calculation of the AP duration (APD) at 30% repolarization (APD_{30}), representing the duration of the AP after early, phase 1 "notch" repolarization, and a calculation of the APD at 60% repolarization (APD_{60}), representing the duration of the AP after the sloped, triangulated plateau (phase 2) typical of the AP morphology. The APD at 90% repolarization (APD_{90}), representing the duration of the AP and indicative of AP refractoriness, was also calculated.

Numerical methods

The system was solved numerically using custom software written in C language. All state variables were updated by means of the forward Euler method. Testing was performed to guarantee that the chosen time step was small enough to ensure convergence of the solutions, and a time step of 10 μs was used to ensure numerical stability and accuracy.

RESULTS

Effects of passive versus active Fb membrane kinetics on hAM electrophysiology

This section examines the effects of coupling Active or Passive Fbs on the AP of the hAM for both Low and High G_{gap}. Results of simulations for a representative number of 2 Fbs are presented.

Fig. 2 shows the effects for a Low G_{gap} (0.5 nS) for 1 Hz pacing. Fig. 2 *A* illustrates the AP of the coupled hAM as compared to the noncoupled control. The hAM is depolarized at rest (+6.9 and +3.3 mV as compared to control, respectively; Fig. 2 *A*, *arrow*), and has decreased APA as compared to the control in Fig. 2 *B* (decrease of 12.4% or 4.6% for Active 1 or Passive models, respectively).

The less-negative RMP is expected to inactivate the Na^+ current, I_{Na}, which is confirmed by an examination of I_{Na} during the first 10 ms of the AP (Fig. 2 *C*). I_{Na} activates earlier for the coupled myocyte, but with decreased $I_{Na,peak}$. This is more marked in the myocyte coupled to Active 1 Fbs. The results reveal a 23.9% vs. 7.6% decrease in $I_{Na,peak}$ as compared to control for a myocyte coupled to Active 1 versus Passive Fb.

Fig. 2 *A* presents distinct repolarization for coupled hAMs as compared to the control. When coupled to Active 1 Fbs, myocyte APD_{30}, APD_{60}, and APD_{90} decrease 10.9%, 31.2%, and 17.3% with respect to the noncoupled control, whereas coupling to Passive Fbs produces only a small delay in phase 3 repolarization (APD_{90} increases by 3.4% as compared to control; see Table S1 and Table S2). An examination of V_{Fb} (Fig. 2 *D*) reveals large differences for Active 1 versus Passive Fbs. Active 1 Fbs exhibit much smaller electrotonic changes, with roughly the same time course of depolarization and repolarization as the myocyte. The electrotonic response is closely linked to G_{gap} and thus to I_{gap}. Fig. 2 *E* illustrates differences in I_{gap} that are observed for a myocyte coupled to either Active 1 or Passive Fbs. Although both Active 1 and Passive Fbs act as current sinks during the AP for the coupled hAM (labeled "1" in Fig. 2 *E*), the peak I_{gap} is 45% greater for a myocyte coupled to Active 1 Fbs. Specifically, Fbs with active K^+ currents act as a stronger current sink during the first ~100 ms of the AP as compared

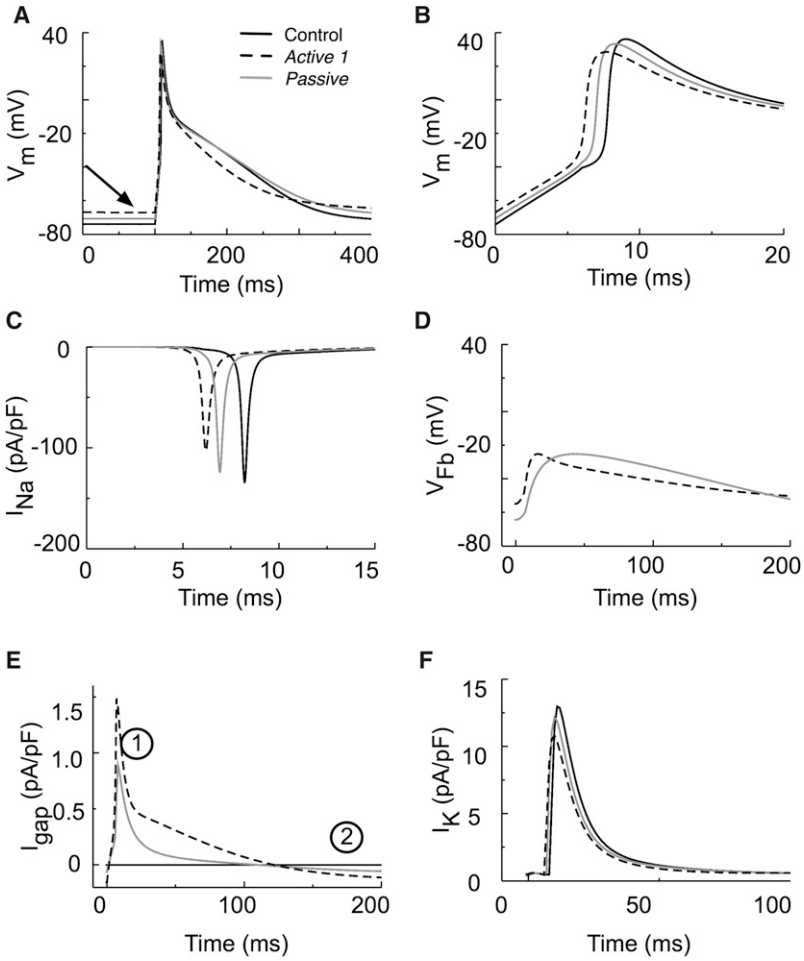

FIGURE 2 AP of a hAM coupled to two *Passive* or *Active 1* Fbs for Low G_{gap} (0.5 nS) as compared to non-coupled hAM. (*A*) hAM AP; arrow indicates differences in RMP. (*B*) Detail of hAM AP during the first 20 ms. (*C*) I_{Na} during the first 10 ms of the AP. (*D*) The transmembrane potential of a coupled Fb, V_{Fb}. (*E*) The gap junctional current, I_{gap}. (*F*) The sum of outward K^+ currents in the hAM, I_K.

to Passive Fbs. After this point in time, coupled Fbs behave as a current source with respect to the myocyte (labeled ''2'' in Fig. 2 *E*). Fig. 2 *F* examines alterations in the net repolarizing current, I_K, of the myocyte as a result of coupling. Note that peak I_K density is decreased slightly for hAMs coupled to Active 1 and Passive Fbs as compared to control, by 18.1% and 5.8%, respectively.

Fig. 3 examines the effects of coupling two Active 1 or Passive Fbs to a hAM via High G_{gap} (8.0 nS) for 1 Hz pacing, underscoring alterations in the AP due to increased G_{gap}. The hAM coupled to Active 1 or Passive Fbs is further depolarized at rest for High G_{gap} (+9.3 and +4.3 mV as compared to control, respectively; Fig. 3 *A*, *arrow*). APA is further decreased (by 23.7% and 13.1% for Active 1 and Passive models, respectively; Fig. 3 *B*). An examination of I_{Na} (Fig. 3 *C*) reveals that coupling to the Active 1 Fb model with a High G_{gap} results in activation 1 ms earlier and a further decrease in $I_{Na,peak}$ (a 42.9% decrease as compared to control). However, activation of I_{Na} is delayed (by 2 ms) when the myocyte is coupled to Passive Fbs, and $I_{Na,peak}$ is decreased 24.5% as compared to control. Activation of I_{Na} is accelerated or delayed at 50% for Active 1 and Passive Fbs (−2 and +2 ms), respectively. Partial inactivation occurs for both Fb models (38.0% and 13.9% inactivation for Active 1 and Passive, respectively, as compared to control).

Phase 2 repolarization of a myocyte coupled to *Active 1* Fbs via High G_{gap} is delayed, whereas phase 3 repolarization is accelerated as compared to control (APD_{30} increases by 55.6%, and APD_{60} and APD_{90} decrease by 22.6% and 13.4% as compared to control).

Fig. 3 *D* shows the profiles of V_{Fb} for Active 1 and Passive Fbs. These profiles follow V_{myo} more closely for High G_{gap} than for Low G_{gap} (Fig. 2 *D*). The increase in G_{gap} allows the stimulus current to be shunted to coupled Fbs, as indicated by ''1'' in Fig. 3 *E*. When Passive Fbs are coupled to a hAM, the low amount of stimulus current available for excitation results in delayed activation of $I_{Na.}$ After excitation, the Fbs act as a current sink (''2'' in Fig. 3 *E*), and then, briefly, as a current source (''3'' in Fig. 3 *E*) for both Active 1 and Passive Fbs. However, the Active 1 Fbs then continue to act as a current sink (''4'' in Fig. 3 *E*), whereas Passive Fbs do not. Finally, Fbs act as a current source (''5'' in Fig. 3 *E*), elevating the RMP of the coupled hAM. Fig. 3 *F* examines the alteration to I_K of the hAM that occurs for both Active 1 and Passive Fbs. The peak I_K density is decreased in the coupled myocyte as compared to control (34.1% and 23.3% decrease for Active

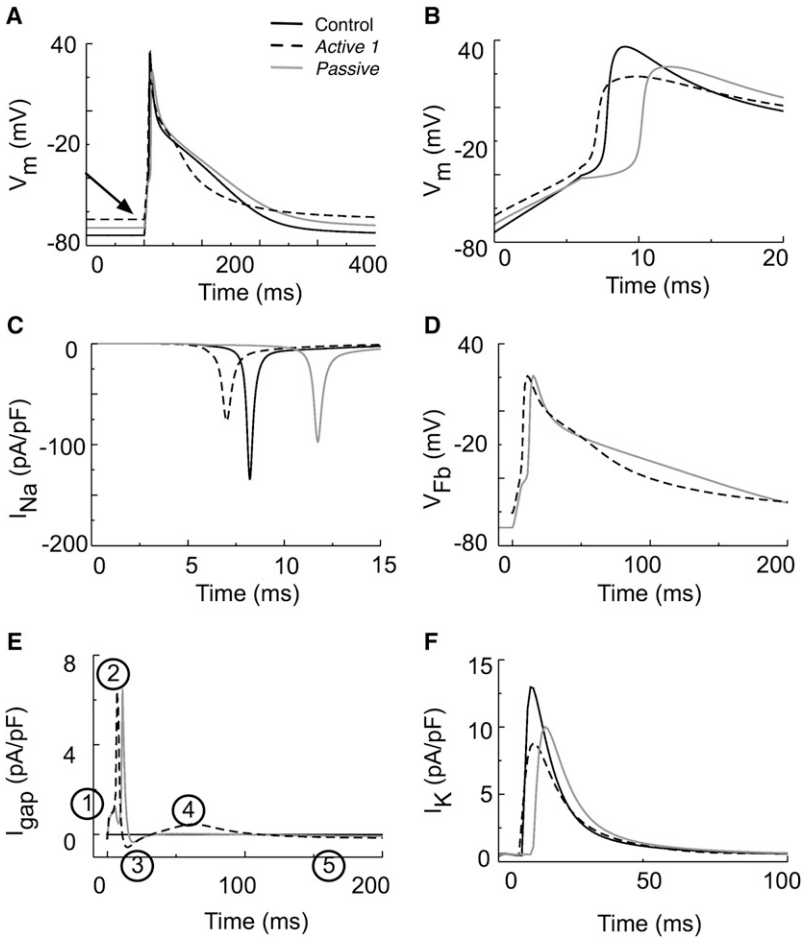

FIGURE 3 AP of a hAM coupled to two Passive or Active 1 Fbs for High G_{gap} (8.0 nS) as compared to non-coupled hAM. (*A*) hAM AP; arrow indicates differences in RMP. (*B*) Detail of hAM AP during the first 20 ms. (*C*) I_{Na} during the first 10 ms of the AP. (*D*) The transmembrane potential of a coupled Fb, V_{Fb}. (*E*) The gap junctional current, I_{gap}. (*F*) The sum of outward K^+ currents in the hAM, I_K.

1 and Passive, respectively). Changes in repolarization that occur when a hAM is coupled to Active 1 or Passive Fbs are further summarized in Table S1 and Table S2.

Effect of the resting potential of the active Fb on hAM AP

Here, the effects of coupling either Active 1 or Active 2 Fbs on the AP of the hAM for both Low and High G_{gap} are examined. Coupling to 2 Fbs is again used to illustrate these findings.

A hAM AP (1 Hz pacing) coupled via a Low G_{gap} to Active 1 or Active 2 Fbs is presented in Fig. 4. As expected, RMP elevation is greater for the myocyte coupled to more depolarized (Active 2) Fbs (+11.9 mV as compared to control; Fig. 4 *A*, *arrow*), resulting in a further decrease in APA, as shown in Fig. 4 *B* (decrease of 24.2% for *Active 2* model as compared to control). I_{Na} activates earlier than control (−3 ms), but I_{Na} is further decreased (47.7% decrease in $I_{Na,peak}$; Fig. 4 *C*).

Fig. 4 *A* reveals repolarization differences for the hAM when coupled to Active 1 versus Active 2 Fbs. Both early and late AP repolarizations of a hAM coupled to Active 1 Fbs are more rapid as compared to control (APD_{30}, APD_{60}, and APD_{90} decrease by 10.9%, 31.2%, and 17.3%, respectively; Table S2). In contrast, coupling to *Active 2* Fbs causes only a small alteration in early repolarization and prolongs late repolarization as compared to control (APD_{30}, APD_{60}, and APD_{90} increase by 11.1%, 0.0%, and 16.3%, respectively; Table S3). The increased depolarization of V_{Fb} (Fig. 4 *D*) for Active 2 as compared to Active 1 Fbs alters the effect of I_{gap} (Fig. 4 *E*) on the myocyte: peak I_{gap} is 22.3% lower early in the AP (''1'' in Fig. 4 *E*), and 30.4% greater later during the AP (''2'' in Fig. 4 *E*). The decrease in peak I_K density is more pronounced for a myocyte coupled to more depolarized (Active 2) Fbs (33.3% decrease as compared to control; Fig. 4 *F*).

Fig. 5 examines the effects of increased G_{gap} when two Active 1 or Active 2 Fbs are coupled to a hAM (1 Hz pacing). High G_{gap} causes further depolarization of the myocyte at rest (+9.3 and +16.8 mV as compared to control for Active 1 and Active 2, respectively; Fig. 5 *A*), as well as more pronounced decreases in myocyte APA (23.7% and 34.0% lower than control for Active 1 and Active 2 models, respectively; Fig. 5 *B*). I_{Na} activation timing is altered and $I_{Na,peak}$ is further decreased (1 and 2 ms earlier than control, and a 42.9% and 63.4% decrease as compared to control for Active 1 and Active 2 models, respectively).

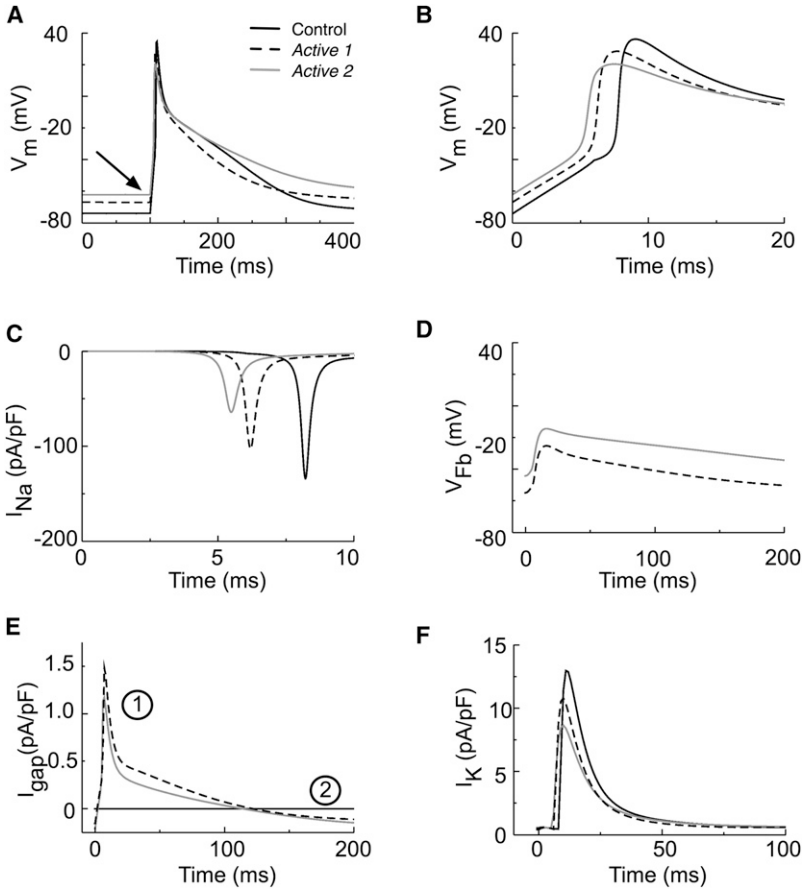

FIGURE 4 AP of a hAM coupled to 2 *Active 1* or *Active 2* Fbs for Low G_{gap} (0.5 nS) as compared to noncoupled hAM. (*A*) hAM AP; arrow indicates differences in RMP. (*B*) Detail of hAM AP during the first 20 ms. (*C*) I_{Na} during the first 10 ms of the AP. (*D*) The transmembrane potential of a coupled Fb, V_{Fb}. (*E*) The gap junctional current, I_{gap}. (*F*) The sum of outward K^+ currents in the myocyte, I_K.

Coupling via High G_{gap} to *Active 2* Fbs (Table S3) prolongs repolarization (APD_{30}, APD_{60}, and APD_{90} increase 61.3%, 13.3%, and 49.5%, respectively, as compared to control). V_{Fb} (Fig. 5 *D*) is less negative for an Active 2 Fb, contributing to distinct I_{gap} for hAMs coupled to Active 2 versus Active 1 Fbs (Fig. 5 *E*). Fig. 5 *F* examines the net repolarization current, I_K, in a coupled hAM; I_K decreased by 48.1% for coupling to Active 2 Fbs as compared to control.

Electrophysiological effect of increased stimulation frequency on the hAM coupled to active Fbs

The effects of coupling either 2 Active 1 or 2 Active 2 Fbs to a hAM paced at either 1 or 4 Hz are examined in panel I of Fig. 6 (High G_{gap}). Fig. 6 *A* shows the changes in the steady-state AP waveform of the control when the stimulation frequency is increased from 1 to 4 Hz. The RMP is elevated by 9.1 mV, resulting in an APA decrease of 19.0% as compared to the 1 Hz case. Due to increased RMP, I_{Na} is partially (36.7%) inactivated for the 4 Hz case as compared to the 1 Hz case. Fig. 6 *B* compares I_{Na} for the two rates: pacing at 4 Hz results in earlier (3 ms) activation and a 41.8% decrease in $I_{Na,peak}$ as compared 1 Hz.

For *Active 1* Fbs, increasing the pacing rate from 1 to 4 Hz further depolarizes the coupled hAM at rest (by 1.7 mV) and results in a ~20% decrease in APA and a 31.9% decrease in $I_{Na,peak}$ as compared to the noncoupled control at the same rate (4 Hz; Fig. 6 *C* (compare with Fig. 5 *C*)). In addition to the effects on Na^+ inactivation, stimulus current now flows to coupled Fbs via I_{gap} (Fig. 6 *E*), reducing the amount of current available for excitation. The AP morphology of the coupled myocyte paced at 4 Hz is triangulated compared to both the noncoupled control and the coupled myocyte paced at 1 Hz (Fig. 6 *C*). The magnitude of current shunted to Fbs is similar for coupled myocytes paced at either 1 or 4 Hz (I_{gap}; Fig. 6 *E*), and I_{gap} further contributes to AP shortening and triangulation in the case of the coupled hAM paced at 4 Hz as compared to the 4 Hz control.

For Active 2 Fbs, 4 Hz pacing results in a maximum diastolic potential of −40.9 mV and a resting depolarization of ~23 mV as compared to the noncoupled control hAM stimulated at the same rate (4 Hz; Fig. 6 *F*). This significant elevation of myocyte RMP leads to almost complete inactivation of I_{Na} (99%). Fig. 6 *G* reveals that $I_{Na,peak}$ has decreased by 98% as compared to the noncoupled control paced at 4 Hz (Fig. 6 *B*), leading to a failed excitation. An examination of I_{gap} (Fig. 6 *H*) confirms that only stimulus current is shunted to the Fbs; after termination of the stimulus, I_{gap} approaches zero, as no AP has been elicited.

A complete picture of the effects of FMC between a hAM and one to three Fbs on hAM excitability is further examined

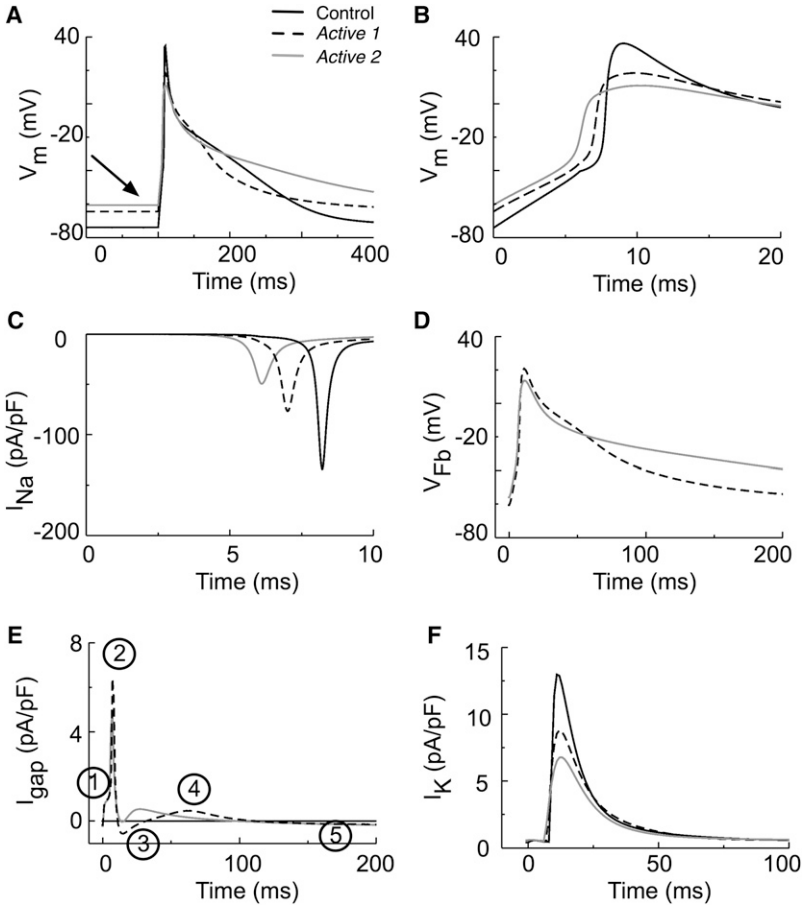

FIGURE 5 AP of a hAM coupled to two *Active 1* or *Active 2* Fbs for High G_{gap} (8.0 nS) as compared to noncoupled hAM. (*A*) hAM AP; arrow indicates differences in RMP. (*B*) Detail of hAM AP during the first 20 ms. (*C*) I_{Na} during the first 10 ms of the AP. (*D*) The transmembrane potential of a coupled Fb, V_{Fb}. (*E*) The gap junctional current, I_{gap}. (*F*) The sum of outward K^+ currents in the myocyte, I_K.

in panel II of Fig. 6. $I_{Na,peak}$ is examined for coupling to both Active 1 (*top row*) and Active 2 (*bottom row*) Fbs, and for stimulation frequencies of 1, 2, and 4 Hz (at *left*, *middle*, and *right*, respectively).

$I_{Na,peak}$ decreases with increases in the number of coupled Fbs and G_{gap}. Coupling any number of Fbs to a hAM via low G_{gap} (0.5 nS) results in a dramatic decrease in excitability as compared to control ($G_{gap} = 0.0$ nS). Increasing G_{gap} from 0.5 to 8.0 nS reveals additional decreases in $I_{Na,peak}$. To investigate the potential effects of further increases in G_{gap}, additional simulations were conducted in which G_{gap} was increased to 16.0 nS. The effects of increasing G_{gap} on excitability become saturated for sufficiently large G_{gap}. Very little additional decrease in $I_{Na,peak}$ occurred with the increase of G_{gap} from 8.0 to 16.0 nS for a given number of coupled Fbs.

Increasing the stimulation frequency of a hAM coupled to Fbs (1–4 Hz) results in at least a 40% reduction of $I_{Na,peak}$ in all cases as compared to the 1 Hz control. The membrane kinetics of coupled Fbs strongly influence $I_{Na,peak}$ in the myocyte when the stimulation rate is increased: Active 2 Fbs coupled to the myocyte paced at 4 Hz result in a majority of cases for which $I_{Na,peak}$ values decrease to $<10\%$ of the noncoupled 1 Hz control value. Clearly, both the pacing rate and the RMP of coupled Fbs contribute to determination of hAM excitability. More depolarized Fb RMP and rapid pacing lead to myocyte RMP elevation, possibly compromising excitability and leading to failed excitation.

Influences on hAM AP waveform

Fig. 7 shows changes in myocyte RMP, APA, APD_{30}, APD_{60}, and APD_{90} as a function of the pacing rate for a hAM coupled to one or three Active 1 or Active 2 Fbs. These are compared with a noncoupled control for both Low (*left*) and High (*right*) G_{gap}.

In general, the RMP of a hAM coupled to Fbs increases and APA decreases as BCL is decreased for both *Active* models and for both G_{gap} values (Fig. 7, *A* and *B*, and *C* and *D*, respectively). Increasing the number of *Active 2* Fbs from one to three depolarizes the myocyte RMP significantly for all rates. For three Fbs coupled via High G_{gap}, RMP depolarization of the hAM is such that it leads to failed excitation at all rates (Fig. 7 *B*). Excitation also fails when one Active 2 Fb is coupled to the myocyte paced at BCL of 250 or 375 ms (Fig. 7 *B*). When an AP is elicited, the decrease in APA as BCL is decreased is more pronounced for coupling to Active 2 Fbs, and for three as compared to one Fb for either Fb model.

In many cases, coupling to Fbs causes only small changes in early repolarization (APD_{30}) of the hAM, which are

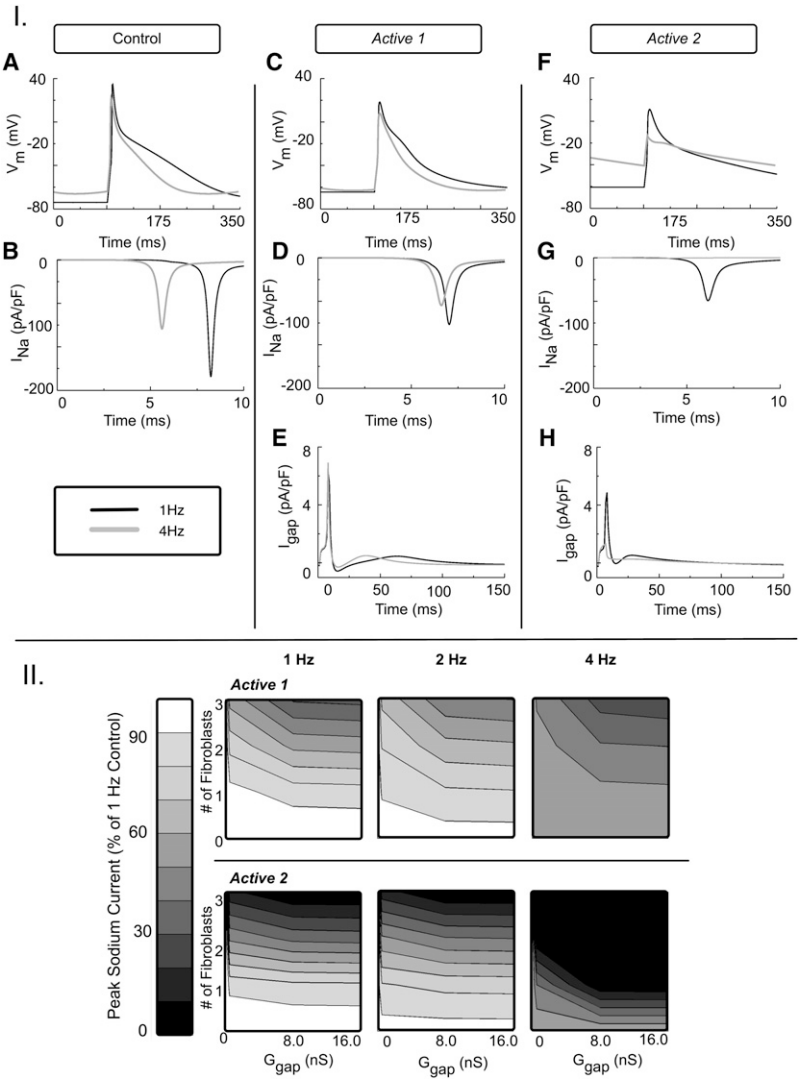

FIGURE 6 Effect of pacing rate on hAM AP and excitability. Panel I: AP of a hAM paced at 1 or 4 Hz and coupled to two *Active 1* (*middle*) or *Active 2* (*right*) Fbs via High G_{gap} (8.0 nS), as compared to noncoupled controls (*left*). (*A*) AP of the noncoupled control, V_{myo}. (*B*) I_{Na} of control. (*C*) AP of coupled hAM,V_{myo} (*Active 1*). (*D*) I_{Na} of coupled hAM (*Active 1*). (*E*) Gap junctional current, I_{gap} (*Active 1*). (*F*) AP of coupled hAM,V_{myo} (*Active 2*). (*G*) I_{Na} of coupled hAM (*Active 2*). (*H*) Gap junctional current, I_{gap} (*Active 2*). Panel II: Effect of hAM coupling to one to three *Active 1* (*top*) or *Active 2* (*bottom*) Fbs at a G_{gap} of 0.0–16.0 nS on $I_{Na,peak}$ for pacing rates of 1, 2, and 4 Hz (*left*, *middle*, and *right*, respectively).

independent of G_{gap}, the pacing rate, and the number of coupled Fbs (Fig. 7, *E* and *F*). Only two cases yield large changes: 1), coupling three Active 2 Fbs to the myocyte doubles APD_{30} as compared to control (Fig. 7 *E*); and 2), when three Active 1 Fbs are coupled to the myocyte, early repolarization is more than twice as slow, on average, for all rates (Fig. 7 *F*).

The duration of the AP after the plateau (APD_{60}) is decreased when the myocyte is coupled to *Active 1* Fbs at all rates, independently of G_{gap}, and is slightly less rate-dependent than the noncoupled control (Fig. 7, *G–J*). However, when three Active 2 Fbs are coupled to a hAM via Low G_{gap}, APD_{60} is almost twice as long as compared to control (Fig. 7 *G*).

AP duration (APD_{90}), which is indicative of refractoriness, is usually decreased when the myocyte is coupled to *Active 1* Fbs at all rates, with overall AP shortening decreasing as the rate is increased (Fig. 7, *I* and *J*). Coupling three Active 1 Fbs to the myocyte via High G_{gap}, however, results in AP prolongation for rapid pacing as compared to the noncoupled control. Coupling the myocyte to Active 2 Fbs always results in AP prolongation (Fig. 7, *I* and *J*).

In summary, coupling between Fbs and a hAM results in RMP elevation of the latter, leading to decreased excitability and APA. Moreover, coupling to Fbs results in diverse effects on myocyte repolarization, including alteration in AP shape and both increased and decreased refractoriness. The degree to which excitability and repolarization are affected varies with the number of coupled Fbs, G_{gap}, the model representing coupled Fbs, and the stimulation rate.

DISCUSSION

The main goal of this study was to obtain insights into the effects of FMC on hAM excitability and AP morphology as a function of 1), G_{gap}; 2), the membrane properties of Fbs; 3), the number of Fbs; and 4), the pacing rate.

The degree to which coupling affects myocyte electrophysiology is highly dependent on the membrane properties of the Fbs and hence the Fb model used. As evidenced by our results,

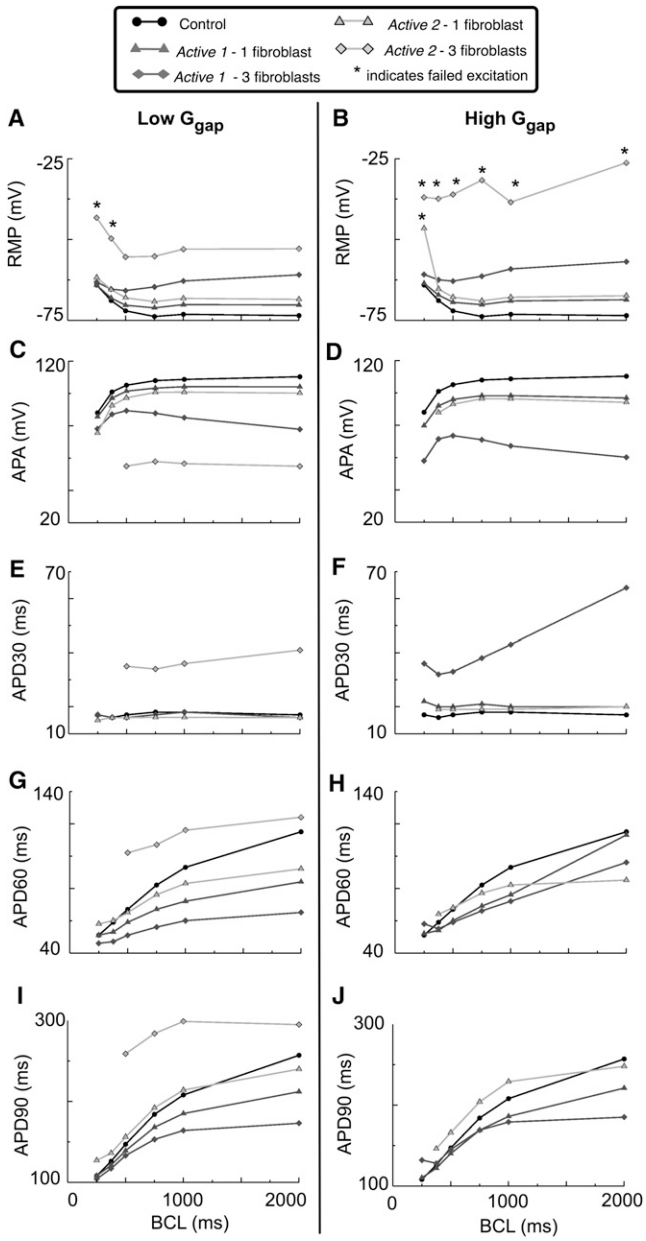

FIGURE 7 Effects of coupling between a hAM and one or three *Active 1* or *Active 2* Fbs on AP characteristics for several rates of stimulation (basic cycle lengths of 250, 375 500, 750, 1000, and 2000 ms). Results for both Low (*left panel*: *A*, *C*, *E*, *G*, and *I*) and High (*right panel*: *B*, *D*, *F*, *H*, and *J*) G_{gap} are shown. Asterisks (*) represent cases of failed excitation in *A* and *B*; these cases are omitted from *C*–*J*. (*A* and *B*) RMP. (*C* and D) APA. (*E* and *F*) APD_{30}. (*G* and *H*) APD_{60}. (*I* and *J*) APD_{90}.

modeling the Fb membrane as a Passive RC circuit does not accurately reproduce the effects of FMC seen in experiments (4,13,18), such as depolarization of the myocyte at rest and excitation disturbances. Our results underscore the need to account for the active membrane properties of Fbs to accurately represent the electrotonic effects of FMC in the atria.

In this study, we employed two novel membrane models of the atrial Fb (see Supporting Material). The resulting RMP of Active 1 and Active 2 Fbs (−47.8 and −31.4 mV, respectively) accurately reproduced measured values (15,16,28). Because a range of RMPs have been measured in isolated Fbs, the use of these two distinct Fb models is essential when exploring the contribution of Fb membrane kinetics to alterations in myocyte AP.

Role of FMC on hAM RMP and excitability

Both the RMP of Fbs and the hAM size relative to that of Fbs (and thus $C_{m,myo}$) are important in determining the depolarization of the coupled hAM at rest. Experimental data from a previous study (13) showed depolarization of neonatal rat ventricular cardiomyocyte strands at rest from ~−78 to ~−50 mV, with maximum depolarization of myocytes occurring when myofibroblasts (myoFbs) interacted with myocytes at a ratio of 2.3:1.

In a recent study investigating coupling between murine ventricular myocytes and Fbs, Jacquemet and Henriquez (19) employed an Fb model with a more negative RMP than either of the Active models used here. In addition, in their study, $C_{m,myo}$ was 153.4 pF, which is ~3 times larger than the 50 pF $C_{m,myo}$ (25) employed in our study. For this reason, the effects on myocyte RMP were much less marked in their model. In fact, their results displayed a maximum depolarization of +8.3 mV for an Fb density of ~30 Fbs ($C_{m,Fb}$ = 6.3pF) per myocyte (19) wherein the coupling conductance used corresponds to a G_{gap} of ~138 nS. In our study, a G_{gap} of 8.0 nS and two Active 1 Fbs resulted in nearly the same hAM RMP elevation. In another study, Sachse et al. (22) modeled the coupling of rat ventricular myocytes ($C_{m,\ myo}$ = 100 pF) to Fbs with an RMP of −58 mV, and found only a small RMP elevation (~ +2 mV) for up to 10 Fbs per myocyte, in contrast to the dramatic effects on hAM RMP in our study. Thus, adequate representation of Fb membrane properties, and incorporation of realistic $C_{m,myo}$ values are essential to assess the effects of FMC on myocyte depolarization at rest.

The electrotonic current flow between Fbs and a myocyte causes depolarization of the hAM at rest, and results in decreased excitability. Our simulations show that coupling to Active 1 Fbs even via Low G_{gap} (0.5 nS) revealed a dramatic decrease in excitability, and the effect was even greater with more depolarized Fb RMPs (Active 2; Fig. 7). A near saturation of this effect, seen at High G_{gap} (8.0 nS; Fig. 7), corresponds to the saturation of effects seen at high intermediate values, as defined by the recent computational study of Jacquemet and Henriquez (18). Sufficient depolarization of the myocyte RMP via coupling to Active 2 Fbs led to complete loss of myocyte excitability. Excitability is also modulated by $C_{m,Fb}$ (see Supporting Material) and stimulation frequency: larger Fbs may increase hAM depolarization and decrease excitability, whereas increased pacing rates lead to decreased excitability via rate-related increases in myocyte RMP.

In addition to the steady-state responses noted above, experiments (30) have revealed dynamic effects on excitability as a result of FMC. Our model of Fb-hAM interaction is able to reproduce spontaneous phenomena, such as delayed afterdepolarizations (DADs) sustained for up to 45 s after rapid pacing protocols (data not shown). However, in this study we focused on a fundamental characterization of the influence of FMC on steady-state hAM behavior. Thus, an exploration of dynamic phenomena was not included here, and will instead be addressed in future work.

Coupling effects on AP waveform and repolarization

Decreased APA with FMC has been predicted by other computational models (19,22). Jacquemet and Henriquez (18), employing a canine atrial AP model (31), found a maximum decrease in APA during FMC of ~33% (~30 coupled Fbs/myocyte, G_{gap} of ~138 nS). The canine model is significantly different from the hAM model used here (25), particularly with respect to representation of repolarization current densities and kinetics. Our results reveal an APA decrease of the same magnitude occurring for a Fb-hAM ratio of 2:1 for a G_{gap} of 8.0 nS, which may more closely represent the range of parameters that are relevant for the human atria. These disparities can also be attributed to differences in $C_{m,myo}$, since the relatively small capacitance of the hAM (50 pF) enhances the influence of coupled Fbs. A comparatively depolarized Fb RMP augments the role of the Fb as a current source and results in further depolarization of the hAM RMP, which reduces I_{Na} availability and decreases APA.

Coupling of the hAM to Fbs in this study also resulted in diverse effects on AP morphology during repolarization. It has been suggested that these effects are also dependent upon specific properties of the myocyte AP (18,19). We found that Fbs functioned as strong current sources at rest, and as both sources and sinks during the AP for coupling via High G_{gap} when we employed a new hAM model (25). Prolongation of repolarization is seen sometimes early in the AP, and plateau is prolonged or shortened depending on both the Fb RMP and number of coupled Fbs.

Alterations in AP shape that occurred with coupling were strongly dependent on Fb RMP in this study. Fbs acted as both current sources and sinks with respect to the coupled myocyte, depending on the AP phase. However, Fbs that are more depolarized at rest (Active 2) were a more powerful current source during early repolarization as compared to Fbs with a more negative RMP (Active 1), which acted as both a current source and sink during the AP plateau. Active 1 Fbs also functioned as a more powerful current sink late in the AP, often increasing the rate of hAM repolarization, as compared to Active 2 Fbs. The FMC study employing a canine atrial model revealed that Fbs acted predominantly as current sinks rather than as sources for similar coupling conductances (18).

Our results also imply distinct alterations in late repolarization and thus the APD and refractoriness of the myocyte with FMC. Briefly, coupling to Active 1 Fbs generally resulted in APD shortening, whereas coupling to Active 2 Fbs resulted in APD prolongation. The effects of Fb coupling on myocyte refractoriness are thus strongly dependent on the Fb RMP. In the study by Jacquemet and Henriquez (18), APD prolongation was witnessed in all cases.

The complex effects of FMC on myocyte repolarization shown by our results, which demonstrate both APD shortening and prolongation, depend on the specific properties of the hAM and the Fb. The prediction of alterations in myocyte repolarization during coupling to Fbs is thus nontrivial and requires consideration of a number of parameters, as well as accurate representation of the AP of the tissue of interest, before one can obtain reasonable insights into such effects.

Study implications

In this study, effects on hAM excitability and repolarization were seen even during FMC via Low G_{gap}, suggesting an influence of Fbs in the human atria even with comparatively high resistances between cells. To elucidate the potential role of Fbs in organ-level arrhythmogenesis, it is important to understand how hAMs are affected by coupling to Fbs. Variation in cell coupling patterns may give rise to a large range of potential electrotonic loads on coupled myocytes; some myocytes may be depolarized as a result of coupling to Fbs, and others in the local area may remain relatively unaffected with respect to the RMP and electrical behavior. Decreased tissue excitability occurring with FMC (as seen here), when combined with local heterogeneity in electrotonic loads, could lead to conduction abnormalities and block, facilitating the development of reentrant arrhythmias in the human atria. The alterations to myocyte repolarization that occur with FMC are also dependent on a number of parameters, including the membrane properties of the Fbs, G_{gap}, and the number of Fbs, which may vary throughout the atria. Additionally, the resulting dispersion of repolarization properties could contribute to the development of an arrhythmogenic substrate in the fibrotic atria.

Recent experimental work has drawn attention to strategies for modulating cardiac excitability based on transfected Fbs (32), and investigations into cell-based therapies for cardiac repair are ongoing (33). Thus, outlining the mechanisms that may be important in FMC is essential to future studies of the behavior of transfected cells and the development of cellular therapies.

Limitations

In this study, we focused on coupling between a hAM and Fbs. However, homologous coupling between Fbs may also occur during structural remodeling of the myocardium. Coupling between adjacent Fbs may be important in tissue models, wherein Fbs can form conduction bridges between

myocyte bundles (12,13). In addition, coupling among Fbs would introduce additional nonlinearity into the coupled system in the case of heterogeneous Fb properties, further altering the global electrophysiological response of the coupled myocyte.

Myofibroblasts may also be involved in FMC in human atria. MyoFbs differ phenotypically from Fbs and feature 5- to 10-fold larger $C_{m,Fb}$. This increase in capacitance suggests that the electrotonic effects on the hAM seen with coupling to Fbs would be enhanced by coupling to MyoFbs.

We did not include local control of Ca^{2+} in our hAM model, which limits our ability to assess the effects of alterations in early repolarization, caused by FMC, on the calcium transient. A decrease in early repolarization currents, such as I_{to}, has been linked to altered density of $I_{Ca,L}$ and subsequent changes in the Ca^{2+} transient, $[Ca^{2+}]_i$ (31,34). Thus, altered early repolarization could result in abnormal excitation-contraction coupling via $I_{Ca,L}$. However, Ca^{2+} cycling in the hAM AP model must be improved to include local control of Ca^{2+} release to facilitate further investigation of the impact of coupling-induced aberrant repolarization on excitation-contraction coupling.

SUPPORTING MATERIAL

Text, three tables, and one figure are available at http://www.biophysj.org/biophysj/supplemental/S0006-3495(09)01356-3.

This study was supported by the National Institutes of Health (grants R01-HL063195, R01-HL082729, and R01-HL067322), National Science Foundation (grant CBET-0601935 to Dr. N. A. Trayanova), Canadian Institutes of Health Research, Heart and Stroke Foundation of Canada, and Alberta Heritage Foundation for Medical Research (Dr. W. R. Giles).

REFERENCES

1. Go, A. S., E. M. Hylek, K. A. Phillips, Y. Chang, L. E. Henault, et al. 2001. Prevalence of diagnosed atrial fibrillation in adults: national implications for rhythm management and stroke prevention: the AnTicoagulation and Risk Factors in Atrial Fibrillation (ATRIA) Study. *JAMA*. 285:2370–2375.
2. Burstein, B., and S. Nattel. 2008. Atrial fibrosis: mechanisms and clinical relevance in atrial fibrillation. *J. Am. Coll. Cardiol.* 51:802–809.
3. Spach, M. S., and P. C. Dolber. 1986. Relating extracellular potentials and their derivatives to anisotropic propagation at a microscopic level in human cardiac muscle. Evidence for electrical uncoupling of side-to-side fiber connections with increasing age. *Circ. Res.* 58:356–371.
4. Camelliti, P., T. K. Borg, and P. Kohl. 2005. Structural and functional characterisation of cardiac fibroblasts. *Cardiovasc. Res.* 65:40–51.
5. Camelliti, P., G. P. Devlin, K. G. Matthews, P. Kohl, and C. R. Green. 2004. Spatially and temporally distinct expression of fibroblast connexins after sheep ventricular infarction. *Cardiovasc. Res.* 62:415–425.
6. Trew, M. L., B. J. Caldwell, G. B. Sands, D. A. Hooks, D. C.-S. Tai, et al. 2006. Cardiac electrophysiology and tissue structure: bridging the scale gap with a joint measurement and modelling paradigm. *Exp. Physiol.* 91:355–370.
7. Kawara, T., R. Derksen, J. R. de Groot, R. Coronel, S. Tasseron, et al. 2001. Activation delay after premature stimulation in chronically diseased human myocardium relates to the architecture of interstitial fibrosis. *Circulation*. 104:3069–3075.
8. Spach, M. S., J. F. Heidlage, P. C. Dolber, and R. C. Barr. 2007. Mechanism of origin of conduction disturbances in aging human atrial bundles: experimental and model study. *Heart Rhythm*. 4:175–185.
9. Pertsov, A. M., J. M. Davidenko, R. Salomonsz, W. T. Baxter, and J. Jalife. 1993. Spiral waves of excitation underlie reentrant activity in isolated cardiac muscle. *Circ. Res.* 72:631–650.
10. ten Tusscher, K. H., and A. V. Panfilov. 2003. Influence of nonexcitable cells on spiral breakup in two-dimensional and three-dimensional excitable media. *Phys. Rev. E Stat. Nonlin. Soft Matter Phys.* 68:062902.
11. Camelliti, P., C. R. Green, I. LeGrice, and P. Kohl. 2004. Fibroblast network in rabbit sinoatrial node: structural and functional identification of homogeneous and heterogeneous cell coupling. *Circ. Res.* 94:828–835.
12. Gaudesius, G., M. Miragoli, S. P. Thomas, and S. Rohr. 2003. Coupling of cardiac electrical activity over extended distances by fibroblasts of cardiac origin. *Circ. Res.* 93:421–428.
13. Miragoli, M., G. Gaudesius, and S. Rohr. 2006. Electrotonic modulation of cardiac impulse conduction by myofibroblasts. *Circ. Res.* 98: 801–810.
14. Kohl, P., P. Camelliti, F. Burton, and G. Smith. 2005. Electrical coupling of fibroblasts and myocytes: relevance for cardiac propagation. *J. Electrocardiol.* 38:45–50.
15. Chilton, L., S. Ohya, D. Freed, E. George, V. Drobic, et al. 2005. K^+ currents regulate the resting membrane potential, proliferation, and contractile responses in ventricular fibroblasts and myofibroblasts. *Am. J. Physiol. Heart Circ. Physiol.* 288:2931–2939.
16. Shibukawa, Y., E. L. Chilton, K. A. Maccannell, R. B. Clark, and W. R. Giles. 2005. K^+ currents activated by depolarization in cardiac fibroblasts. *Biophys. J.* 88:3924–3935.
17. Kohl, P., and P. Camelliti. 2007. Cardiac myocyte-nonmyocyte electrotonic coupling: implications for ventricular arrhythmogenesis. *Heart Rhythm*. 4:233–235.
18. Jacquemet, V., and C. S. Henriquez. 2008. Loading effect of fibroblast-myocyte coupling on resting potential, impulse propagation, and repolarization: insights from a microstructure model. *Am. J. Physiol. Heart Circ. Physiol.* 294:H2040–H2052.
19. Jacquemet, V., and C. S. Henriquez. 2007. Modelling cardiac fibroblasts: interactions with myocytes and their impact on impulse propagation. *Europace*. 9 (Suppl 6):vi29–vi37.
20. MacCannell, K. A., H. Bazzazi, L. Chilton, Y. Shibukawa, R. B. Clark, et al. 2007. A mathematical model of electrotonic interactions between ventricular myocytes and fibroblasts. *Biophys. J.* 92:4121–4132.
21. Jacquemet, V. 2006. Pacemaker activity resulting from the coupling with nonexcitable cells. *Phys. Rev. E Stat. Nonlin. Soft Matter Phys.* 74:011908.
22. Sachse, F. B., A. P. Moreno, and J. A. Abildskov. 2008. Electrophysiological modeling of fibroblasts and their interaction with myocytes. *Ann. Biomed. Eng.* 36:41–56.
23. Kamkin, A., I. Kiseleva, K. D. Wagner, A. Pylaev, K. P. Leiterer, et al. 2002. A possible role for atrial fibroblasts in postinfarction bradycardia. *Am. J. Physiol. Heart Circ. Physiol.* 282:H842–H849.
24. Kiseleva, I., A. Kamkin, P. Kohl, and M. J. Lab. 1996. Calcium and mechanically induced potentials in fibroblasts of rat atrium. *Cardiovasc. Res.* 32:98–111.
25. Maleckar, M. M., J. L. Greenstein, W. R. Giles, and N. A. Trayanova. 2009. K^+ current changes account for the rate dependence of the action potential in the human atrial myocyte. *Am. J. Physiol. Heart Circ. Physiol.* Jul 24 [Epub ahead of print].
26. Rook, M. B., A. C. van Ginneken, B. de Jonge, A. el Aoumari, D. Gros, et al. 1992. Differences in gap junction channels between cardiac myocytes, fibroblasts, and heterologous pairs. *Am. J. Physiol.* 263: C959–C977.
27. Kohl, P., A. Kamkin, I. Kiseleva, and D. Noble. 1994. Mechanosensitive fibroblasts in the sino-atrial node region of rat heart: interaction with cardiomyocytes and possible role. *Exp. Physiol.* 79:943–956.

28. Kamkin, A., I. Kiseleva, and G. Isenberg. 2003. Activation and inactivation of a non-selective cation conductance by local mechanical deformation of acutely isolated cardiac fibroblasts. *Cardiovasc. Res.* 57: 793–803.

29. Hund, T. J., J. P. Kucera, N. F. Otani, and Y. Rudy. 2001. Ionic charge conservation and long-term steady state in the Luo-Rudy dynamic cell model. *Biophys. J.* 81:3324–3331.

30. Miragoli, M., N. Salvarani, and S. Rohr. 2007. Myofibroblasts induce ectopic activity in cardiac tissue. *Circ. Res.* 101:755–758.

31. Sah, R., R. J. Ramirez, and P. H. Backx. 2002. Modulation of Ca(2+) release in cardiac myocytes by changes in repolarization rate: role of phase-1 action potential repolarization in excitation-contraction coupling. *Circ. Res.* 90:165–173.

32. Feld, Y., M. Melamed-Frank, I. Kehat, D. Tal, S. Marom, et al. 2002. Electrophysiological modulation of cardiomyocytic tissue by transfected fibroblasts expressing potassium channels: a novel strategy to manipulate excitability. *Circulation.* 105:522–529.

33. Yankelson, L., Y. Feld, T. Bressler-Stramer, I. Itzhaki, I. Huber, et al. 2008. Cell therapy for modification of the myocardial electrophysiological substrate. *Circulation.* 117:720–731.

34. Greenstein, J. L., and R. L. Winslow. 2002. An integrative model of the cardiac ventricular myocyte incorporating local control of Ca^{2+} release. *Biophys. J.* 83:2918–2945.